HYDROLOGICAL PROCESSES
Hydrol. Process. **28**, 823–836 (2014)
Published online 21 November 2012 in Wiley Online Library
(wileyonlinelibrary.com) DOI: 10.1002/hyp.9633

Melt water driven stream and groundwater stage fluctuations on a glacier forefield (Dammagletscher, Switzerland)

Jan Magnusson,[1]* Florian Kobierska,[1] Stephan Huxol,[2] Masaki Hayashi,[3] Tobias Jonas[1] and James W. Kirchner[4,5]

[1] *WSL Institute for Snow and Avalanche Research SLF, Flüelastrasse 11, CH-7260 Davos Dorf, Switzerland*
[2] *Eawag: Swiss Federal Institute of Aquatic Science and Technology, CH-8600 Dübendorf, Switzerland*
[3] *Department of Geoscience, University of Calgary, 2500 University Drive NW, Calgary, Alberta, T2N 1N4, Canada*
[4] *Swiss Federal Institute for Forest, Snow, and Landscape Research WSL, CH-8903 Birmensdorf, Switzerland*
[5] *Department of Environmental Sciences, Swiss Federal Institute of Technology, ETH, CH-8092 Zürich, Switzerland*

Abstract:

In many mountain regions, large land areas with heterogeneous soils have become ice-free with the ongoing glacier retreat. On these recently formed proglacial fields, the melt of the remaining glaciers typically drives pronounced diurnal stream level fluctuations that propagate into the riparian zone. This behaviour was measured on the Damma glacier forefield in central Switzerland with stage recorders in the stream and groundwater monitoring wells along four transects. In spite of the large groundwater stage variations, radon measurements in the near-stream riparian zone indicate that there is little mixing between stream water and groundwater on daily time scales. At all four transects, including both losing and gaining reaches, the groundwater level fluctuations lagged the stream stage variations and were often damped with distance from the stream. Similar behaviours have been modelled using the diffusion equation in coastal regions influenced by tidal sea level variations. We thus tested the ability of such a model to predict groundwater level fluctuations in proglacial fields. The model reproduced several key features of the observed fluctuations at three of four locations, although discrepancies also arise due to non representative input data and model simplifications. Nevertheless, calibration of the model for the individual transects yielded realistic estimates of hydraulic diffusivities between the stream and groundwater monitoring wells. We conclude that studying diurnal groundwater fluctuations can provide important information about the subsurface hydrology of alpine watersheds dominated by glacier melt.

KEY WORDS glacier melt; proglacial field; stream-groundwater interactions; diurnal fluctuations; diffusion model

Received 21 October 2010; Accepted 11 October 2012

INTRODUCTION

Downstream of glaciers, melt water typically flows through braided streams on a glacial floodplain, with potentially significant subsurface water fluxes through riparian till deposits (Ward *et al*., 1999). Both the surface and groundwater flow influence the chemical, physical, and biological processes taking place on glacier forefields (Warburton, 1992; Fairchild *et al*., 1999). However, the characteristics of groundwater flow in such heterogeneous environments with irregular topography and moraine-like soils are still poorly understood (Roy and Hayashi, 2009). In this study, we analysed how periodic stream level variations caused by glacier melt propagate into the riparian zone of the Damma glacier forefield in the central Swiss Alps.

In many glacierized watersheds, diurnal stream stage fluctuations caused by glacier melt likely propagate into the groundwater of the riparian zone. In other environments, similar groundwater fluctuations have been studied in detail, for example adjacent to streams fed by snowmelt (Loheide and Lundquist, 2009) and in the vicinity of regulated rivers (e.g. Francis *et al*., 2010). Although diurnal stage fluctuations are likely to drive stream-groundwater interactions in glacial forefields, these interactions have rarely been studied. The scarcity of such studies can be attributed to the difficulty of monitoring groundwater levels in remote glacierized watersheds (Cooper *et al*., 2002).

For a proglacial field site in Svalbard, Cooper *et al*. (2002, 2011) observed that diurnal fluctuations in groundwater stage were damped and lagged compared to variations in stream stage driven by glacier melt. They found increasing groundwater levels during snowmelt and a flood event; otherwise, the subsurface water levels remained stable throughout their study. In Alaska, Crossman *et al*. (2011) measured daily stage variations in groundwater-fed streams close to a glacial floodplain. Throughout the summer, they observed increasing groundwater levels in piezometers near the streams due to increasing infiltration of river water from the floodplain. Otherwise, near-stream water level observations on proglacial field sites seem scarce, and, here, we report results for one such field site in high alpine terrain.

Simple analytical models have adequately predicted tide-driven groundwater fluctuations in coastal aquifers

*Correspondence to: Jan Magnusson, WSL Institute for Snow and Avalanche Research SLF, Flüelastrasse 11, CH-7260 Davos Dorf, Switzerland
E-mail: magnusson@slf.ch

(Nielsen, 1990, Raubenheimer *et al*., 1999 and Montalto *et al*., 2007). They reproduce the basic properties of diffusive wave propagation, namely a nearly linear increase in time lag and an exponential damping of the wave's amplitude with distance. In a sub-alpine riparian zone, Loheide and Lundquist (2009) showed that these diffusion models can also predict diurnal snowmelt-induced groundwater fluctuations. Their study site was a flat meadow with relatively homogeneous soil. However, glacier forefields usually have highly heterogeneous soils and irregular topography. Thus, the question remains whether groundwater fluctuations in glacier forefields propagate according to the same analytical models.

The aims of this study are to (1) present observations of seasonal and diurnal relationships between stream stages and riparian groundwater levels on an alpine glacier forefield, (2) examine whether the diurnal fluctuations in stream and groundwater levels cause substantial mixing between the two water bodies, (3) test whether the diurnal fluctuations of groundwater level in the riparian zone can be explained by diffusive propagation of stream level fluctuations, and (4) examine whether we can use the diffusion model to estimate realistic hydraulic properties of the heterogeneous sediments on the forefield.

THEORY OF WAVE PROPAGATION

In many studies, fluctuations in groundwater levels caused by periodic variations at a boundary, for example due to tidally driven sea level variations, have been simulated using different forms of the diffusion equation (e.g. Montalto *et al*., 2007; Sun, 1997). Such models predict an exponential damping and a linear increase in time lag of the propagating wave with distance away from the boundary. In the case of one-dimensional wave propagation over a flat base, the linear diffusion equation can describe the variations in groundwater stage:

$$\frac{\partial h}{\partial t} = D\frac{\partial^2 h}{\partial x^2} \tag{1}$$

where h is the transient perturbation of hydraulic head (m) from its mean value, x is the distance normal to the stream (m), t is the time (days), and D is the hydraulic diffusivity (m^2/day). The hydraulic diffusivity is given by:

$$D = \frac{Kb}{S} \tag{2}$$

where K is the hydraulic conductivity (m/day), b is the saturated thickness of the aquifer (m), and S is the specific yield (dimensionless). We assume that the specific yield equals the porosity of the sediments. This assumption may overestimate S, but it represents a reasonable approximation for the relatively coarse sediments found near proglacial streams. Because Equation (1) is linear, the propagation of groundwater fluctuations can be analysed independent of other hydrological processes. For example, horizontal drainage flow can be modelled separately from the propagation of water level variations, and the results can be included in the solution by the principle of superposition (Montalto *et al*., 2007). The stream stage fluctuations can be represented with a Fourier series:

$$h(0,t) = \sum_{n=1}^{m} A_n \sin(\omega_n t + \varphi_n) \tag{3}$$

where A_n is the amplitude (m), ω_n is the angular frequency (rad/day), and φ_n is the phase angle (rad). A solution for the diffusion equation with this type of boundary condition (Dirichlet boundary condition on a semi-infinite domain) is given by Equation (4) (see Montalto *et al*., 2007).

$$h(x,t) = \sum_{n=1}^{m} A_n \exp\left(-\sqrt{\frac{\omega_n}{2D}}x\right) \sin\left(\omega_n t - \sqrt{\frac{\omega_n}{2D}}x + \varphi_n\right) \tag{4}$$

The model presented above relies on several assumptions: (1) homogeneous hydraulic properties of the sediments and no transmission losses across the streambed, (2) an infinite straight stream adjacent to the aquifer, (3) a horizontal and impermeable aquifer base, (4) water stage fluctuations that are small compared to the thickness of the saturated zone, and (5) no recharge to or evaporation from the aquifer (c.f. Loheide and Lundquist, 2009).

STUDY SITE AND DATA

The Damma glacier forefield

The Damma glacier forefield in the central Swiss Alps (46°38.177` N 08°27.677` E) covers an area of approximately 0.5 km^2 and an elevation range from 1950 to 2050 m a.s.l. (Figure 1). The proglacial field is bounded upstream by a debris-covered dead-ice body (separated from the glacier, which has retreated further up the valley headwall) and laterally by two large side moraines dating from approximately 1850 (the end of the Little Ice Age). The topography of the watershed is characterized by high alpine terrain with steep slopes (up to nearly 80°). The topography of the forefield itself is uneven, with slopes ranging between roughly 3° and 16°. The main stream exits the dead-ice body and follows a braided path through the forefield. A side stream originating from the northern part of the glacier joins the main stream from the north-west. The hydrological regime of the study area is dominated by runoff generation from the seasonal snow cover and the glacier (Magnusson *et al*., 2011). The average annual precipitation at the site is approximately 2400 mm.

Site instrumentation

We measured water levels at four transects along the main stream channel, each consisting of one stream stage recorder (housed in a perforated tube) and two groundwater monitoring wells situated perpendicular to the stream (Figure 1). The wells consisted of fully screened plastic tubes 6 cm in diameter, extending to depths between 60 and 130 cm. The well spacing varied between

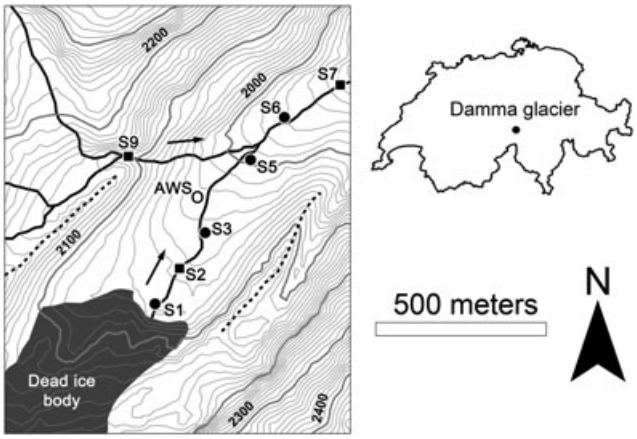

Figure 1. The Damma glacier forefield in central Switzerland. The forefield is bounded by a dead-ice body and two large side moraines from the Little Ice Age (indicated with dotted black lines). The four sampling sites of stream and groundwater level (solid circles numbered S1, S3, S5, and S6) are located along the main stream (black lines, with arrows showing the flow direction). The discharge gauging stations are located such that they measure the water flowing in from the north and south (solid squares denoted S9 and S2, respectively) and out of the forefield (solid square denoted S7). The automatic weather station (AWS) is located in the middle of the forefield. Terrain elevation is shown by 10 m contour intervals

2 and 5 m. Water levels were recorded using non-vented pressure sensors (Hobo U20 Water Level Logger with 0.14 cm resolution and 0.3 cm accuracy according to the manufacturer's specification). The stream stages were measured at a 2-min sampling interval, and the groundwater stages were measured at a 5-min sampling interval. The measurements were averaged to 10-min values. The absolute pressure readings were adjusted for atmospheric pressure variations (measured at site S7 on the forefield, using the same type of pressure sensor). The four transects are denoted S1, S3, S5, and S6 in increasing order downstream (see Figure 1). The in-stream water level recorders are denoted $S1_{stream}$, $S3_{stream}$, $S5_{stream}$, and $S6_{stream}$, and the near-stream and more distant groundwater recorders are denoted $S1_{near}$ and $S1_{far}$, $S3_{near}$ and $S3_{far}$, and so on.

The groundwater monitoring sites were selected to represent different characteristics of the glacier forefield (Figure 2; Table I): S1) flat ground with a rather straight stream section of variable width; S3) flat ground with a meandering stream reach with highly variable cross sections; S5) steep slopes facing slightly toward the stream with a relatively straight stream section; and S6) intermediate slopes and variable stream cross section.

We continuously recorded discharge at three locations, capturing the water flowing into (sites S2 and S9) and out of (site S7) the forefield. At these sites, water levels were recorded with the same devices as described above (Hobo U20 Water Level Logger with 2-min sampling interval, averaged to 10-min values). The measured water levels were converted to discharges using a rating curve measured by dilution gauging. For more details about the stream gauging, see Magnusson *et al*. (2012).

Meteorological conditions were recorded at an automatic weather station situated on the glacier forefield (Figure 1). Hourly precipitation rates were measured using a tipping bucket rain gauge (ARG100, Campbell Scientific) with a precision of 0.20 mm according to the manufacturer.

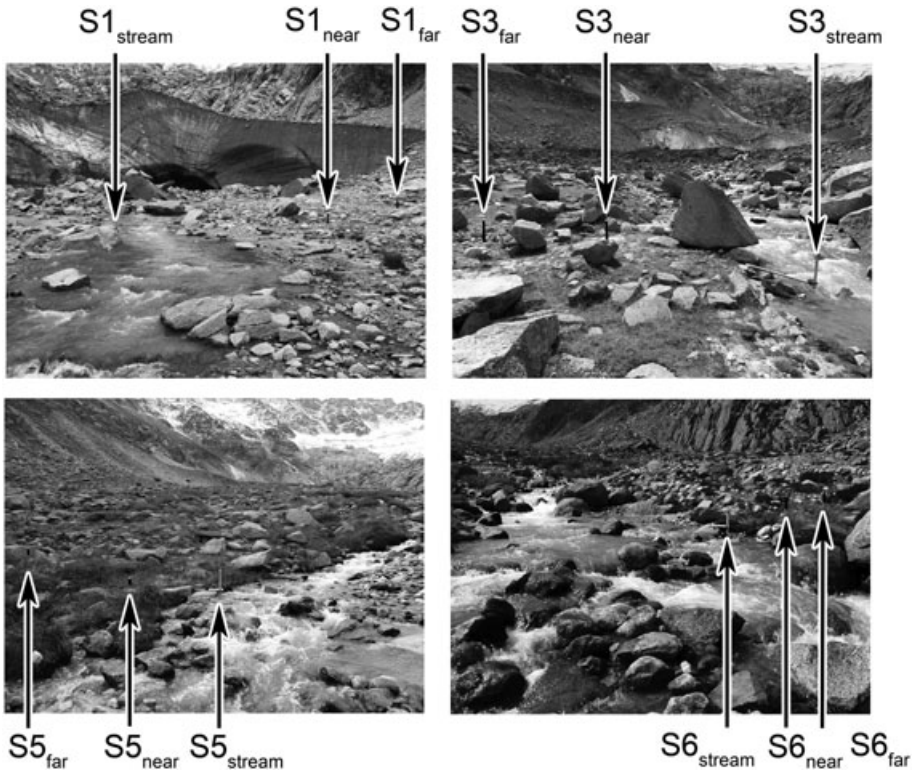

Figure 2. Photos (looking upstream) showing the four measurement transects, each equipped with one stage recorder in the stream and two stage recorders in groundwater monitoring wells

Table I. Distances between stream and groundwater monitoring wells measured from field surveys and the approximate surface slope parallel and perpendicular to the streams

Location	Distance between the stream and near groundwater well (m)	Distance between the stream and far groundwater well (m)	Surface slope parallel to the stream (°)	Surface slope perpendicular to the stream (°)
S1	5	10	2	2
S3	4	6	4	2
S5	2	4	11	4
S6	2	4	6	6

Aquifer and sediment properties

Despite large moraine boulders covering the forefield, the sediments are mainly constituted of cobbles and sand with some silt and minor amounts of clay (Bernasconi and BigLink consortium, 2011). We carried out both refraction seismic surveys and electrical resistivity surveys on four transects near sites S1, S3, and S6 (unpublished data) using similar methods to Langston *et al*. (2011). The preliminary results suggest that the glacial till is at least 10 m thick. Unfractured granitic bedrock appears to lie more than 20 m below the surface. The transition between glacial till and bedrock appears to consist of a porous material, which could be either compacted sediments (glacial till) or fractured bedrock.

The hydraulic conductivity of the glacial till was measured with slug tests in the groundwater monitoring wells following the standard procedure (e.g. Butler, 1998), with data analysis by the method of Bouwer and Rice (1976). This method assumes that the well screen is completely submerged below the water table. This assumption is not met in the study site, introducing some uncertainty in estimated conductivity values due to the effects of draining and filling of pores in the aquifer material and variable screen length during the tests (Binkhorst and Robbins, 1998, Aragon-Jose and Robbins, 2011). To estimate the degree of uncertainty resulting from the partially submerged screen, rising and falling head tests were conducted for each of the two wells in the study transects, resulting in four values of hydraulic conductivity per transect. However, at site S3, the length of the submerged screens were short (~0.2 m), and only falling head tests could be performed, which may have constrained the range of measured hydraulic conductivities at this location. The estimated hydraulic conductivities of all sites varied between 1 and 45 m/day (Table II) and were similar to those measured in glacial tills elsewhere (Hinton *et al*., 1993, Boulton and Zatsepin, 2006).

The average glacial till porosity of 0.25 was obtained from 14 samples taken from the upper layers (5–15 cm depth) of the sediments on the forefield (Smittenberg *et al*., 2012). This porosity is within the range of values found for glacial tills on other field sites (ASCE, 1996).

OBSERVED WATER LEVEL RECORDS

Seasonal discharge and water level trends

During dry weather periods, the regular variability in glacier melt rates produced a clear diurnal pattern in stream discharge (Figure 3a). For such periods, the highest flows of the day occurred around noon and could be more than twice as a high as the low flows in the morning. Similar diurnal fluctuations in stream discharge have been observed in many watersheds with snowmelt and glacier melt runoff regimes (e.g. Jobard and Dzikowski, 2006, Loheide and Lundquist, 2009) and are also widespread in regulated rivers (e.g. Francis *et al*., 2010). The clear diurnal fluctuations in discharge driven by glacier ablation were only interrupted by rain events, which were associated with the highest runoffs we recorded.

Near the dead-ice body (site S1), the water levels in the far-stream monitoring well were 11–69 cm higher than in the stream, indicating subsurface water flow towards the channel (Figure 3b). The groundwater levels showed a slow declining trend over the season, but rain events caused the water levels to rise sharply, with a fast recession following. The fast rise in stage is likely due to a thin unsaturated zone (between 23 and 94 cm thick), which allows rain water to quickly percolate through the

Table II. Lowest and highest measured hydraulic conductivity along the different transects, including the geometric average hydraulic conductivity

Location	Lowest measured hydraulic conductivity (m/day)	Highest measured hydraulic conductivity (m/day)	Average measured hydraulic conductivity (m/day)
S1	1.0	17.3	6.6
S3	2.6	11.3	5.4
S5	40.6	44.9	42.3
S6	2.9	38.9	16.3

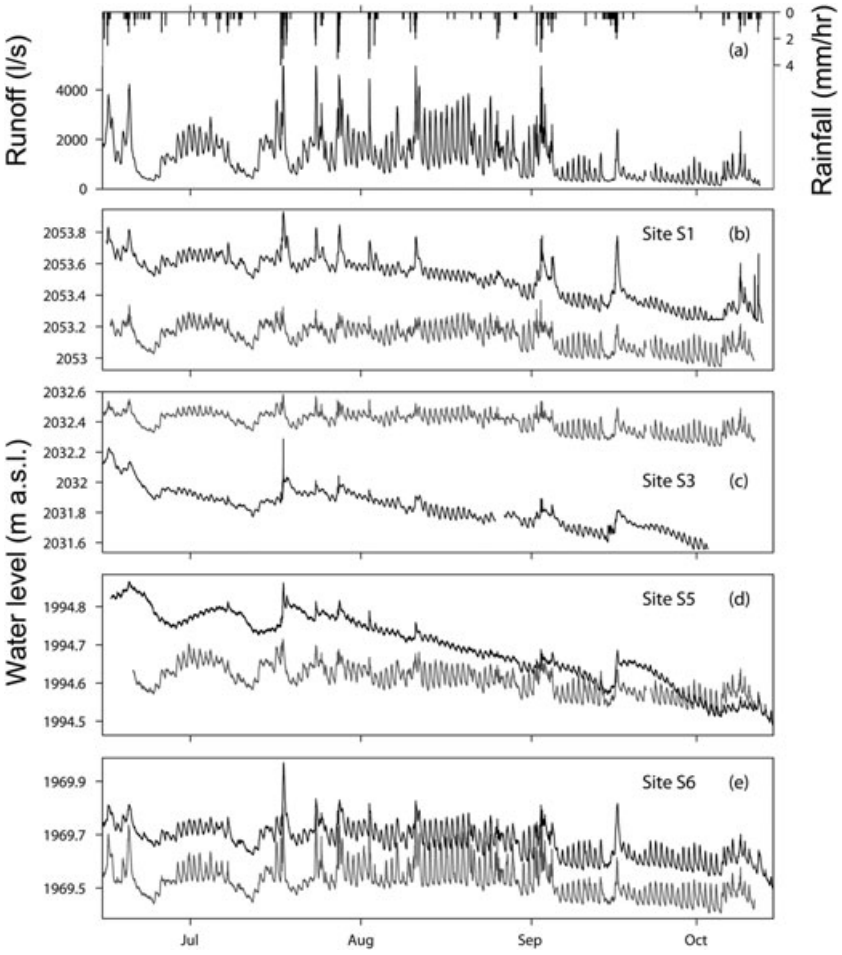

Figure 3. Precipitation, stream, and groundwater time series for the 2009 field season. (a) Precipitation and stream discharge (measured at site S2). (b–e) Stream stage (gray lines) and groundwater levels (black lines) in far-stream monitoring wells at each transect

sediments. During dry weather periods, the groundwater levels showed clear diurnal cycles.

In the middle of the forefield (site S3), the groundwater levels in the far-stream monitoring well were 26–85 cm below the stream level, suggesting a losing reach (Figure 3c). The water levels in the well declined during the season, even though the hydraulic gradient suggested that stream water infiltrates into the riparian zone. Supposedly, the infiltration rates should increase with time due to a steepening hydraulic gradient (from roughly 0.06 to 0.11 m/m). Rainfalls influenced the groundwater stages with less pronounced peaks than at site S1 and S6, perhaps due to a relatively thick unsaturated zone (between 52 and 126 cm thick). The groundwater levels displayed pronounced diurnal cycles during glacier ablation.

At the steepest location (site S5), the hydraulic gradient was directed toward the stream most of the time at the far-stream monitoring well (Figure 3d). Groundwater levels declined over the season, and fluctuated with stream stage during dry weather conditions. Well levels hardly reacted to rainfall in spite of a thin unsaturated zone (between 9 and 48 cm thick). However, in mid September, the groundwater levels increased sharply after rainfall but without a rapid recession following. In beginning of July and in mid September, the groundwater levels showed a delayed response to variations in stream flow. This behaviour suggests that a delayed groundwater flow from uphill influenced the measurements, similar to observations in sloping terrain elsewhere (Rohde and Seibert, 2011).

At the farthest downstream transect (site S6), groundwater levels in the far-stream well remained more constant throughout the season than at the other sites (Figure 3e). Similar to measurements at site S1, groundwater levels responded to rain events by rising rapidly with a fast recession following (thickness of the unsaturated zone varied between 60 and 108 cm). The hydraulic gradient indicates groundwater flow towards the stream. The largest diurnal water level fluctuations were recorded at this site, suggesting a high connectivity between the stream and groundwater stage in the monitoring well.

Diurnal water level fluctuations

To analyze the daily water level fluctuations in more detail, we selected three eight-day intervals with dry weather conditions. The accumulated precipitation, measured with the automatic weather station located on the forefield, was between 0 and 4 mm during these periods. Note that none of the monitoring wells were flooded

during the three dry weather periods, even at the high stream flows caused by glacier melt. We numbered the periods as follows:

T1: 11 to 19 August 2009
T2: 22 to 30 September 2009
T3: 26 June to 4 July 2010

Average discharge varied between the periods (1880, 440, and 2080 l/s measured at site S2 during T1, T2, and T3, respectively), and roughly followed the pattern in average air temperatures (T1: 13.2 °C; T2: 9.0 °C; T3: 13.4 °C recorded at the weather station). In the following, we analyze the amplitudes of the stream and groundwater level fluctuations observed during the three dry weather periods, as well as the time lag and correlation between the time series (Table III). The time lags and correlation coefficients were determined by a cross-correlation analysis for the individual periods. The water level data is presented in Figure 4, in which the three graphs for each location and period are arranged so that the well (or stream) with the highest hydraulic head is placed at the top and the lowest at the bottom.

At site S1, the groundwater fluctuations lagged behind the stream stage variations, and the time lag increased with distance from the stream during all periods (Table III). During periods T1 and T2, the high optimum correlation coefficients (r_{max}) showed that the propagating wave was not deformed between the stream and groundwater measurements. This indicates that only the adjacent stream stage variations as recorded by the pressure transducer influenced the groundwater fluctuations, and that the component frequencies (Fourier modes) of the diurnal stage variations were equally damped over the travel distance of the propagating wave. For periods T1 and T2, the amplitudes of the groundwater fluctuations were damped compared to the stream stage variations. During period T3, on the other hand, the amplitudes showed a peculiar pattern with rather modest fluctuations at $S1_{near}$ but very large amplitudes at $S1_{far}$. Moreover, the stage in $S1_{near}$ did not rise above a certain threshold level (Figure 4c). During this period, the groundwater level was only about 12 cm below the surface at $S1_{near}$ at high stages. For all study periods, water level fluctuations at site S1 propagated against the direction of the hydraulic gradient.

At site S3, the time lag between the stream and groundwater fluctuations increased with distance from the channel and was the largest among the sites (Table III). We observed a slightly stronger correlation between the stream and groundwater level variations in $S3_{near}$ than $S3_{far}$. The increasing time lag and decreasing correlation with distance from the channel are consistent with diffusive wave propagation. At the same time, the diurnal groundwater cycles were larger in $S3_{far}$ than in $S3_{near}$, which appears inconsistent with wave propagation by diffusion. However, in both monitoring wells, the diurnal stage variations were smaller than in the stream. Several factors could explain the higher amplitudes in $S3_{far}$ than $S3_{near}$, including (1) heterogeneities in hydraulic conductivity, (2) different hydraulic connections between the stream and the two monitoring wells, and (3) processes other than one-dimensional and horizontal diffusion influencing wave propagation. The steep hydraulic gradient, which is directed away from the stream, is an indication of low-conductivity sediments between stream and monitoring wells (Cardenas, 2010).

At site S5, only the stage observations in the far-stream monitoring well showed clear diurnal fluctuations (Figure 4g–i). These water table variations, which had low amplitudes compared to the other sites, lagged behind the stream stage fluctuations (Table III). Water levels in the monitoring wells were both lower ($S5_{near}$) and higher ($S5_{far}$) than in the stream. To examine the groundwater flow direction in detail, we performed tracer experiments by injecting fluorescent dyes into both monitoring wells. Because of the steep down-valley gradient, these tracers were found downstream (~1 m for $S5_{near}$ and ~4 m for $S5_{far}$) in small springs on the stream bank after a short time (after ~1 min for $S5_{near}$ and after ~20 min for $S5_{far}$), indicating a gaining stream reach. Water levels in $S5_{near}$ are typically around 30 cm below those in the adjacent stream channel and exhibit very

Table III. Ratios between amplitudes of groundwater and stream level fluctuations (A_{ratio}), and the time lag determined by cross-correlation analysis (τ) with the associated optimum correlation coefficient (r_{max}). In most locations, the amplitudes were damped landward and the time lag increased. Monitoring well $S5_{near}$ was omitted from the analysis since those water level measurements did not display any pronounced diurnal fluctuations. Missing/omitted values are denoted with dashes

Location	A_{ratio}			τ (min)			r_{max}		
	T_1	T_2	T_3	T_1	T_2	T_3	T_1	T_2	T_3
$S1_{stream} \rightarrow S1_{near}$	0.62	0.51	0.49	60	70	90	0.98	0.98	0.79
$S1_{stream} \rightarrow S1_{far}$	0.46	0.55	1.88	130	120	130	0.97	0.97	0.90
$S3_{stream} \rightarrow S3_{near}$	0.57	-	0.70	100	-	110	0.97	-	0.87
$S3_{stream} \rightarrow S3_{far}$	0.82	0.50	0.72	160	220	140	0.94	0.90	0.81
$S5_{stream} \rightarrow S5_{near}$	-	-	-	-	-	-	-	-	-
$S5_{stream} \rightarrow S5_{far}$	0.24	0.38	0.47	90	50	90	0.87	0.93	0.76
$S6_{stream} \rightarrow S6_{near}$	1.08	1.51	1.04	20	30	10	0.98	0.98	0.96
$S6_{stream} \rightarrow S6_{far}$	0.66	0.93	0.61	40	40	30	0.97	0.98	0.95

T_1 - 11 Aug. 2009 to 19 Aug. 2009. T_2 - 22 Sep. 2009 to 30 Sep. 2009. T_3 - 26 Jun. 2010 to 4 Jul. 2010. For distances between stream and groundwater monitoring wells, see Table I.

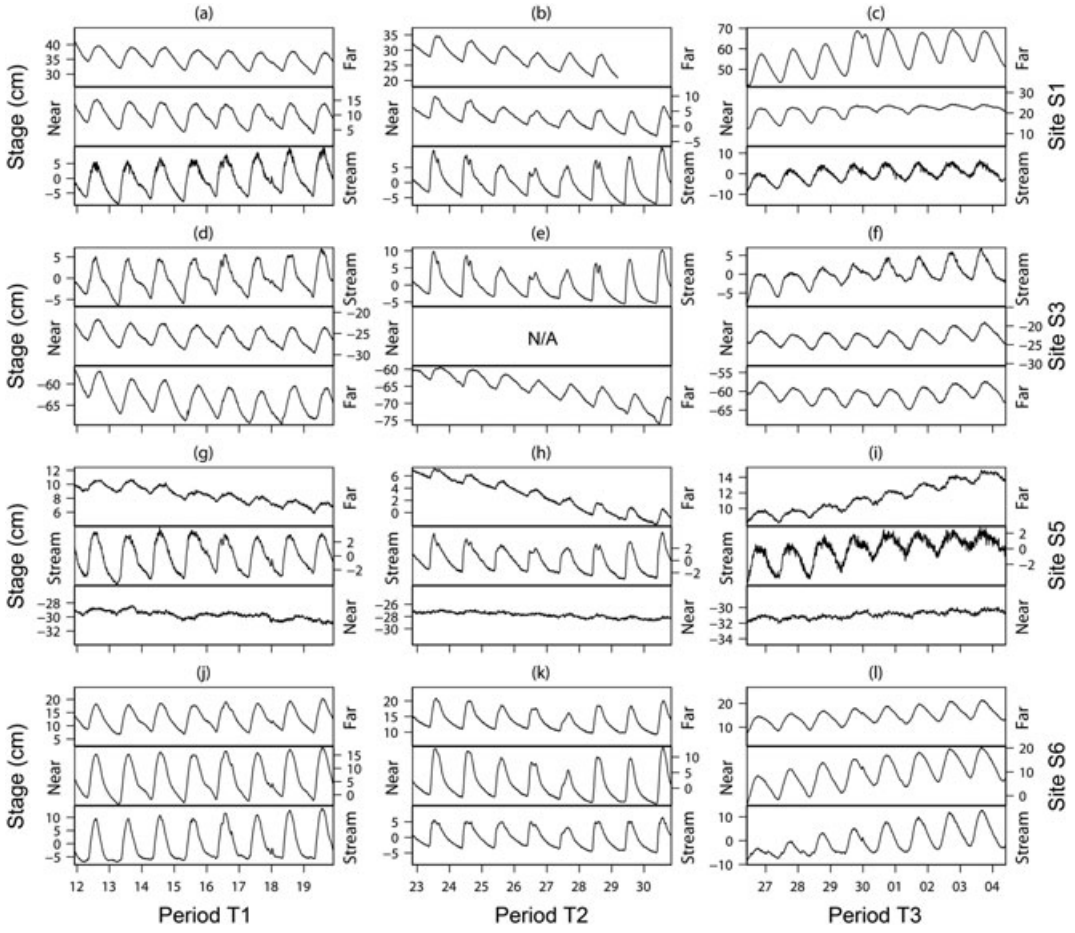

Figure 4. Stream and groundwater levels measured during three dry weather periods. For clarity, we present the stage records (stream stage record, near-stream monitoring well, and far-stream monitoring well measurements) on separate vertical axes. Reported stages are expressed relative to the average stream water level. The three graphs for each location and period are arranged so that the well (or stream) with the highest hydraulic head is placed at the top and the lowest at the bottom. Some data are missing due to sensor failures and wells drying up ($S1_{far}$ during period T2 and $S3_{near}$ during period T2)

small diurnal fluctuations (<1 cm in the well versus >5 cm in the stream). From these observations, we infer that $S5_{near}$ is largely isolated from the adjacent stream channel and its stage fluctuations. Although $S5_{near}$ drains rapidly to small springs on the stream bank roughly 1 m downstream of the transect (and roughly 3 cm below the well itself), the steep hydraulic gradient from the adjacent slope (Figures 1 and 2) and fast groundwater flow apparently inhibit the propagation of stage fluctuations from the springs to the well. At this steeper location, the processes influencing the propagation of stream stage fluctuations into the riparian zone seem even more complex than at the remaining sites.

At site S6, the stream stage fluctuations propagated rapidly to the monitoring wells, with time lags increasing with distance from the stream (Table III). The faster wave propagation observed at this site (roughly 6 m/h) than at the other locations (less than about 5 m/h) indicates sediments with comparably high hydraulic conductivity. The diurnal groundwater fluctuations showed both higher ($S6_{near}$) and lower ($S6_{far}$) amplitudes than observed in the stream. At least for the near-stream monitoring well, the observed amplitudes suggest that the groundwater fluctuations are (a) driven by larger stage variations in the stream than measured by the in-stream transducer and/or, (b) influenced by a more complex flow than described by diffusion (Equation (1)). The stream at this site is less braided than at the remaining locations and also accommodates higher discharges due to the contributions from the channel draining the north-western part of the watershed (the averaged runoff at site S7 is 62 % higher than at site S2). This could imply that the larger stream has a greater influence on the riparian flow dynamics than the smaller streams (S1, S3, and S5) do, which is consistent with the larger stage fluctuations at this site. The stream and groundwater fluctuations were similar, resulting in high correlation coefficients. This similarity suggests that the diurnal stream and groundwater stage fluctuations were closely coupled.

We also analyzed the relationships between water level fluctuations among the four in-stream stage recorders installed at the groundwater monitoring sites. The time lag between the sites, as determined by cross-correlation analysis, was short, varying between 10 and 20 min from $S1_{stream}$ to $S6_{stream}$. Note also that the observed stream level variations in the channel draining the north-western part of the watershed (site S9) were in phase with the measurements in the main channel and therefore did not significantly alter the phase of the diurnal cycle at $S6_{stream}$. Although the time lags between the four stream locations were small, the amplitudes of the diurnal cycles

varied by a factor of 2.3 to 3.1 (depending on the period examined) among the four groundwater monitoring sites. This shows that streambed morphology, turbulence effects, and the braiding of the streams have a strong impact on the amplitude of the diurnal water level fluctuations but not on their timing.

CHARACTERIZING STREAM-GROUNDWATER INTERACTIONS USING ESTIMATES OF RESIDENCE TIMES

The variations of groundwater levels in the riparian zone do not necessarily imply transport of water to or from the stream. Likewise, the hydraulic gradient measured perpendicular to the streams does not fully describe the groundwater flow direction, due to a significant down-valley gradient on the forefield. To estimate timescales of exchange between the stream and riparian groundwater, we measured the concentration of the radioactive noble gas radon (^{222}Rn, half-life 3.82 days) in the groundwater monitoring wells and the stream on two occasions following dry weather periods. This measurement method has been used in many groundwater studies in lowland regions; see Hoehn and Vongunten (1989) and Vogt *et al.* (2010) for a more detailed method description. Similar to these authors, we used a Rad7-radon detector (Durridge Co.) to measure ^{222}Rn in 250 ml samples. The radon concentration in each sample was measured four times, yielding the mean radon concentration and a standard deviation (Table IV).

When nearly radon-free stream or melt water infiltrates into the aquifer, it gradually becomes enriched with radon, generated by the decay of radium present in the aquifer material. If no gas transfer occurs in the groundwater, the radon concentrations increase with time. After about four half-lives (~15 days), the radon concentrations in the groundwater reach a steady state as the decay rate comes into equilibrium with the production rate. With a known equilibrium concentration, measurements of the radon concentration along a groundwater flow path give an estimate of the time that has passed since the water was in contact with the atmosphere (Hoehn and Vongunten, 1989). However, because all sampled groundwater wells are situated near the stream, it was not possible to determine the equilibrium concentration of radon. Therefore, we cannot determine the absolute radon age of the water, but we can nonetheless use the radon concentration as a relative travel-time indicator.

The groundwater samples collected from the transects at the gaining reaches of the stream showed an increase in radon concentration (average of the two sampling events) with distance from the dead-ice body at three measurement locations (52.3, 59.4, and 86.5 Bq/l at S1, S5, and S6, respectively). The highest radon concentrations (66.0 – 98.0 Bq/l) were measured in the most downstream sampling site (S6). The lowest radon concentrations (8.5 – 17.4 Bq/l, indicating relatively young groundwater) were measured at transect S3, a losing reach where the groundwater levels were lower than the stream stage. The radon measurements and the hydraulic gradient are both consistent with infiltration of stream water into the aquifer at this sampling site.

At the gaining stream reaches (S1, S5, and S6), groundwater radon concentrations were higher than in the stream (>30.4 Bq/l compared to 0.40 Bq/l of the stream water), even in the groundwater monitoring wells near the stream. We thus conclude that, locally and on a daily basis, large volumes of water are not exchanged between the riparian zone and the stream. In the particular case of well $S5_{near}$, its radon concentrations are comparable to those in other groundwater wells (for example site S1) even though its water table is some 30 cm below the adjacent stream level, suggesting that it is hydraulically isolated from the adjacent stream channel, consistent with its small water-table fluctuations shown in Figure 4g–i.

MODELLING GROUNDWATER FLUCTUATIONS

The three-dimensional groundwater flow field can be complex around our monitoring wells. Nevertheless, one-dimensional diffusive wave propagation may still have a strong influence on how stream stage fluctuations spread into the groundwater of the riparian zone. Therefore, we

Table IV. ^{222}Rn concentrations (with standard deviation of four replicate measurements), measured on two different days following dry weather conditions. The high concentrations indicate limited mixing between groundwater and stream water, in spite of the large water level fluctuations in the stream and groundwater monitoring wells. The stream was sampled near site S2. Missing values are denoted with dashes

Location	19 July 2010		6 September 2010	
	Concentration (Bq/l)	Standard deviation (Bq/l)	Concentration (Bq/l)	Standard deviation (Bq/l)
Stream	0.40	0.16	-	-
$S1_{near}$	49.5	2.2	94.2	3.2
$S1_{far}$	35.1	2.4	30.4	0.8
$S3_{near}$	8.5	1.8	11.5	2.0
$S3_{far}$	12.0	1.5	17.4	1.0
$S5_{near}$	47.2	1.5	56.8	5.0
$S5_{far}$	56.8	2.7	76.8	4.7
$S6_{near}$	66.0	8.8	97.3	5.6
$S6_{far}$	84.5	7.4	98.0	2.4

examine whether the simple one-dimensional diffusion model (Equation (1)) can reproduce the observed groundwater fluctuations using measured parameters. This approach can provide a useful means to examine the stream-groundwater interaction in the remote and rugged site, where the necessary data for a complex three-dimensional model are lacking. In this study, some assumptions of the one-dimensional diffusion model are met (e.g. small water table fluctuations compared to the aquifer thickness) whereas others are questionable (e.g. straight stream and homogeneous glacial till). Whether the assumptions are violated is not always clear; for example, it may be possible to treat the sediments as homogeneous over the typical length scale of our transects.

General modelling procedure

The groundwater fluctuations were simulated using the following procedure (see panels in Figure 5):

1. *Isolating diurnal water level fluctuations* – The records were detrended in order to better isolate diurnal water level fluctuations. Thus, the linear trends of the dry weather records were removed from the time series (the same periods as analysed above).
2. *Determining model input* – We then approximated the stream stage fluctuations with a Fourier series of sine functions (see Equation (3)). The coefficients of the sine functions (A_n, ω_n, and φ_n) were extracted with a Fourier analysis and later used as model input (see step 3). For this analysis, we multiplied the detrended stream level records with a windowing function to make them periodic (Tukey window with alpha coefficient equal 0.125). The Fourier decomposition covered frequencies between 1/8 per day and 72 per day, given by the sampling frequency and the length of the data record.
3. *Modelling groundwater fluctuations* – We simulated the groundwater fluctuations with the diffusion model (Equation (4)) using the input determined in the previous step (the coefficients A_n, ω_n, and φ_n). Note that we neglect the influence of the boundary at the far end of the aquifer (i.e. the mountain wall) because the distance between the stream channel and the monitoring wells (2–10 m) is much smaller than the distance between the stream and the mountain wall (at least 100 m).

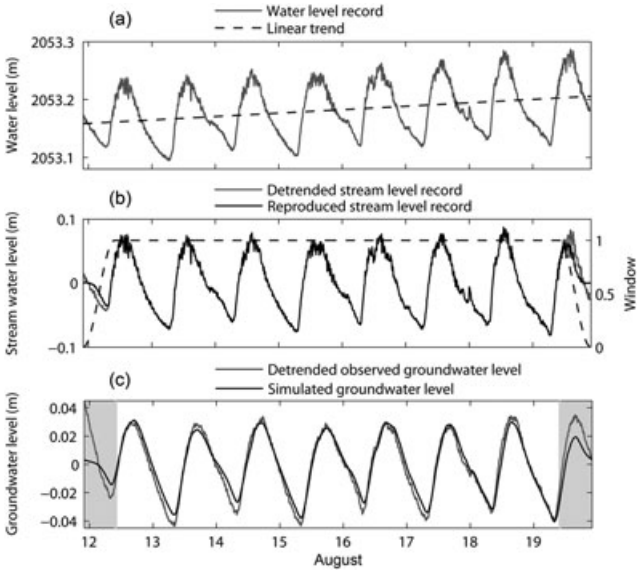

Figure 5. Illustration of the modelling procedure using data from site S1: (a) detrending water level time series to clarify diurnal water level fluctuations; (b) windowing the stream water level time series for model input; and (c) modelling groundwater fluctuations. Note that the windowed stream level record depicted in the middle panel (b), which is used to drive the model, matches the detrended stream level record very closely except at the beginning and at the end of the time series

In the following section, we analyze the observed groundwater fluctuations by means of simulations using the diffusion model with measured parameters and input data (see 'Forward modelling method and results' below). Then, we test whether realistic values for the hydraulic diffusivity of the glacial till can be estimated through calibration of the diffusion model (see 'Inverse modelling methods and results' below).

Forward modelling method and results

Three cases were simulated by using different hydraulic conductivities of the sediments:

K_{ave} – The geometric average measured hydraulic conductivity at each site (Table II).
K_{low} – The lowest measured hydraulic conductivity at each site (Table II).
K_{high} – The highest measured hydraulic conductivity at each site (Table II).

In the simulations, we use the average measured porosity (0.25) and assume that the thickness of the saturated zone is 20 m, based on the geophysical results (as described in the section 'Study site and data'). The true saturated zone thickness may deviate from our assumed value, but the relative uncertainty in the depth of the saturated zone is probably much lower than the spread in measured hydraulic conductivity for most transects (Table II). We assume that the groundwater fluctuations propagate along the measured distance between the stream and monitoring wells (Table I). Supposedly, complex groundwater flow close to the irregular stream channel will influence the far-stream observations less than the near-stream measurements. Therefore, we only show simulation results for the far-stream monitoring wells (Figure 6, Table V).

For site S1, the observed groundwater fluctuations were much better reproduced by the simulations using the two higher observed hydraulic conductivities (K_{ave} and K_{high}) than the lowest measured conductivity (Figure 6a–b, Table V). The simulations suggest that hydraulic conductivities in the range of K_{ave} and K_{high} are representative for the glacial till between the stream and the monitoring well, provided that the remaining parameters are valid. The results also indicate that the diffusion model is a reasonable description of the wave propagation for the

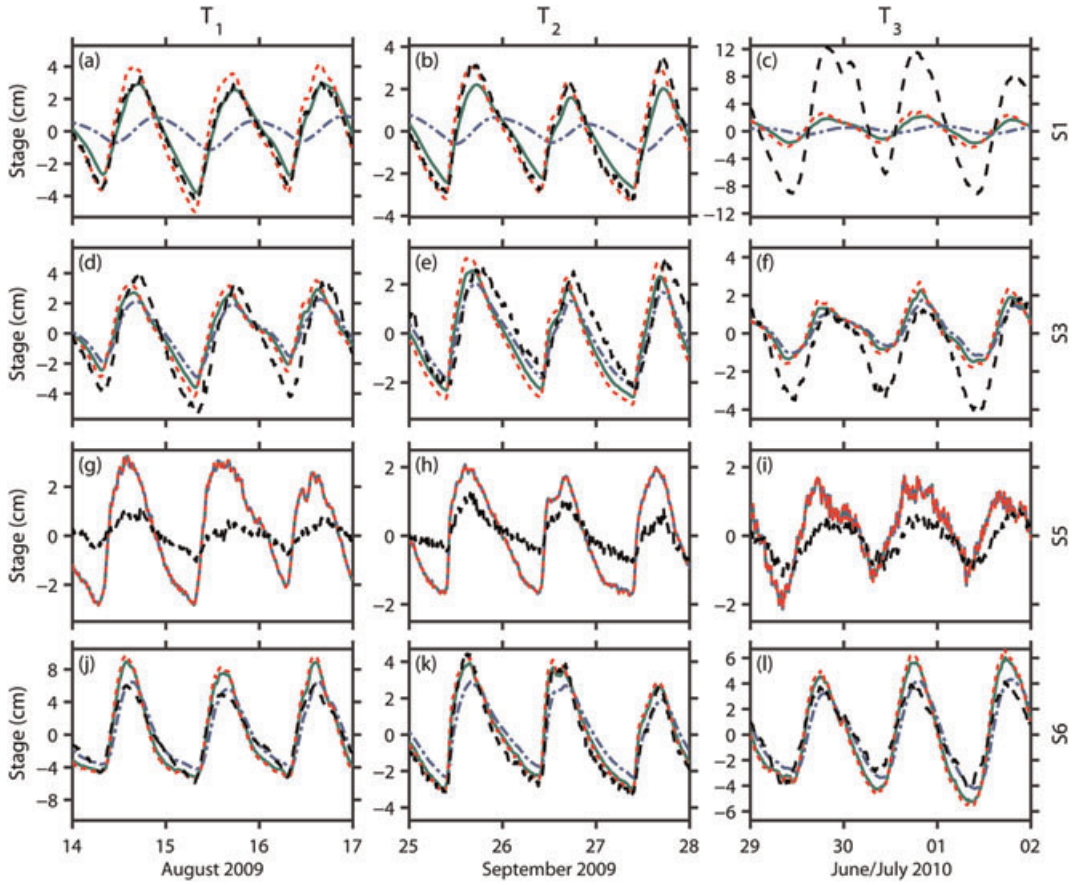

Figure 6. Measured groundwater fluctuations (black dashed line) and simulated stage variations for the farthest groundwater wells at the four transects, using three different hydraulic conductivity values: K_{ave} (green solid line), K_{high} (red dotted line), and K_{low} (blue dash-dotted line)

Table V. Diffusion model simulation results using measured input data and parameters. Ratio between the amplitude of simulated and observed groundwater level fluctuations (A_{sim}/A_{obs}), simulated and observed (within parenthesis) time lags between the stream and groundwater fluctuations (τ), and the correlation coefficient (r_{max}) between the observed and simulated groundwater fluctuations. The table shows the result for the far-stream monitoring wells and the three different cases of hydraulic conductivity. The time lags were obtained by cross-correlation analysis. The goodness-of-fit measures were only determined for the flat part of the windowing function used in the modelling (the white region in the lowest panel of Figure 5). For this reason, the observed time lags sometimes deviate from the values presented in Table III.

Location	Case	A_{sim}/A_{obs}			τ (min)			r_{max}		
		T_1	T_2	T_3	T_1	T_2	T_3	T_1	T_2	T_3
S1	K_{low}	0.25	0.21	0.06	430 (130)	410 (110)	440 (150)	0.28	0.28	0.32
	K_{ave}	0.87	0.74	0.21	150 (130)	130 (110)	170 (150)	0.98	0.99	0.94
	K_{high}	1.19	1.00	0.29	90 (130)	70 (110)	100 (150)	0.97	0.97	0.93
S3	K_{low}	0.52	0.81	0.53	140 (160)	130 (200)	150 (140)	0.96	0.87	0.82
	K_{ave}	0.67	1.03	0.68	100 (160)	80 (200)	100 (140)	0.92	0.78	0.81
	K_{high}	0.79	1.22	0.82	70 (160)	50 (200)	70 (140)	0.87	0.69	0.77
S5	K_{low}	3.16	2.20	2.01	20 (90)	10 (50)	0 (110)	0.81	0.90	0.69
	K_{ave}	3.17	2.20	2.02	20 (90)	10 (50)	0 (110)	0.81	0.90	0.69
	K_{high}	3.18	2.21	2.04	20 (90)	10 (50)	0 (110)	0.81	0.90	0.69
S6	K_{low}	0.92	0.66	0.88	90 (40)	80 (40)	100 (40)	0.95	0.94	0.92
	K_{ave}	1.22	0.87	1.18	40 (40)	30 (40)	40 (40)	0.98	0.98	0.95
	K_{high}	1.31	0.93	1.27	20 (40)	10 (40)	30 (40)	0.97	0.97	0.95

T_1 - 11 Aug. 2009 to 19 Aug. 2009. T_2 - 22 Sep. 2009 to 30 Sep. 2009. T_3 - 26 Jun. 2010 to 4 Jul. 2010.

conditions prevailing during period T1 and T2. However, for period T3, the simulations did not reproduce the amplitudes of the observed groundwater fluctuations. During this period, the groundwater levels were very shallow as noted above and may have created ponding on the surface in local depressions. These very shallow groundwater levels may have influenced the propagation of the groundwater fluctuations.

For site S3, the timing of the groundwater fluctuations was better reproduced by the simulations using the lowest measured hydraulic conductivity (K_{low}), whereas simulations using K_{ave} and K_{high} instead matched the observed amplitudes more closely (Table V). Inaccurate forcing data can partly explain the difference between the simulated and observed groundwater fluctuations. The amplitude of the diurnal cycle can vary substantially along the channel due to changes in the cross-sectional geometry, and the groundwater wells are likely to respond to stage variations originating from many points along the stream, not just the point where the stream stage recorder is located. For the low-conductivity case, the diffusion model would reproduce the groundwater fluctuations better if forced by larger stream stage variations than measured by the pressure transducer. However, this is not possible for the two higher conductivity cases (K_{ave} and K_{high}), since the modelled timing of the groundwater fluctuations does not change with the amplitude of the forcing data (see Equation (4)). At losing stream reaches, complex flow patterns can occur close to the channel due to heterogeneities in the streambed (Irvine *et al.*, 2012). These processes are not included in the diffusion model. Such influences can also contribute to the difference between simulation and observation and can potentially also explain the change in model performance between the two first and the last study periods (compare Figure 6d–e with 6f).

For the steepest location (site S5), the diffusion model largely overestimated the amplitudes of the groundwater fluctuations (Figure 6g–i), but underestimated their timing (Table V). At this site, the results suggest that the model is an inadequate description of the wave propagation process. The fast groundwater flow, as measured by the tracer experiments, directed towards the stream but slightly downstream of the monitoring wells, likely influenced the propagation of stream fluctuations into the riparian zone. We found velocities up to ~300 m/day determined by the first arrival in springs on the stream bank of a fluorescent dye injected into the $S5_{far}$ groundwater monitoring well (for a description of the tracer experiments see section 'Observed water level fluctuations'). In addition, the very low amplitudes of the water table fluctuations in the near-stream monitoring well also suggest that some small region with low hydraulic diffusivity is impending the penetration of hydraulic waves into the riparian zone. These results clearly show that the diffusion model fails in steeply sloping terrain with fast groundwater flow and heterogeneous sediments.

For site S6, the simulations using the average measured hydraulic conductivity (K_{ave}) reproduced the timing of the groundwater fluctuations better than those using either the high or low conductivity values (Table V). The K_{ave} and K_{high} simulations matched the measured amplitudes of the groundwater fluctuations closer during period T2 than the other periods, which were better depicted by the K_{low} simulations (Figure 6j–l). For period T2, the average stream and groundwater stage was roughly 10 to 13 cm lower than during the two other periods. Thus, the variations in model performance may be caused by the varying hydraulic connection between the stream and the monitoring well, as stream and groundwater levels rise and fall. An alternative explanation is that the groundwater level variations may be driven by a more complex subsurface flow at this site than can be described by the simple one-dimensional diffusion model.

Inverse modelling method and results

Figure 6 indicates that the water level fluctuations predicted by the diffusion model are fairly sensitive to the assumed hydraulic diffusivity. The model also simulates the observed data reasonably well when the conditions are favourable (e.g. S1 and S6 during periods T1 and T2). Therefore, it appears promising to use an inverse modelling approach to obtain estimates of hydraulic diffusivity through calibration. We used a non-linear optimization algorithm (Lagarias *et al.*, 1998) to find the hydraulic diffusivity providing the highest correlation coefficient between the observed and simulated groundwater levels. This objective function is insensitive to the amplitude of the time series, and the best-fit value of hydraulic diffusivity only depends on the shape and timing of the signal. This approach was chosen since the timing of the stream stage fluctuations varied much less between the locations than the amplitudes did (see description in section 'Observed water level records'). The correlation coefficient was only determined for the flat part of the windowing function used in the modelling (the white region in the lowest panel of Figure 5). We assume that the stream stage fluctuations propagate along the measured distance between the stream and monitoring well (Table I), although the precise location of the hydraulic connection to the stream is unknown. We excluded site S5 from the analysis since the results above suggest that the diffusion model is inadequate for this location.

The hydraulic diffusivities obtained by calibration varied between the sites and study periods (Table VI). The differences between the periods may reflect changes in the hydraulic connection at different stream stages, or unmodelled three-dimensional flow effects. The calibration produced higher diffusivities for the two gaining stream

Table VI. Hydraulic diffusivities obtained by calibration of the diffusion model using measurements from the far-stream monitoring wells and independent estimates of hydraulic diffusivity computed from observations of hydraulic conductivity, sediment porosity, and saturated aquifer thickness. The range in calibrated hydraulic diffusivities represents the differences between the study periods. The variations in the independent estimates of hydraulic diffusivities depend on the variations in estimated hydraulic conductivities for the individual transects (Table II)

Location	Calibrated hydraulic diffusivity (m^2/day)	Independent estimates of hydraulic diffusivity (m^2/day)
S1	674–736	80–1384
S3	114–248	208–904
S6	859–1156	232–3112

reaches (sites S1 and S6) than the losing stream channel (site S3). The variations between the sites likely depend on differences in specific sediment properties. For comparison, we estimated a range of hydraulic diffusivities from the minimum and maximum measured hydraulic conductivity (Table II), the average observed porosity (0.25) and the assumed thickness of the saturated zone (20m) using Equation (2). The calibrated hydraulic diffusivities presented above are mostly within the range of the independent estimates (Table VI).

DISCUSSION

The groundwater levels declined slowly over the season at three sites, indicating a net loss of groundwater in the riparian zone. Even during periods with increasing stream flow during glacier ablation, neither stream infiltration nor subsurface flows from uphill could compensate for flows out of the riparian zone. Melting snow appears to recharge the water levels in the near-stream riparian zone during spring. In both 2009 and 2010, the snowmelt period lasted until the first week of June at the automatic weather station. In some places, melting snow patches also lasted longer than at the meteorological station. Thus, even close to the streams, it seems that snowmelt is an important component of the subsurface water balance apart from stream-groundwater exchanges and recharges due to rainfall.

In our study site, the radon concentration measurements showed that the diurnal water level fluctuations did not result in large local mixing between stream water and groundwater on daily time scales. This is contrary to the findings elsewhere (Fritz and Arntzen, 2007, Loheide and Lundquist, 2009), showing that snowmelt-induced or regulated periodic river stage fluctuations caused a large volume of water to be pumped in and out of riparian sediments. The mentioned studies were performed in relatively flat landscapes compared to our more steeply sloping proglacial valley. Our results suggest that for certain slopes and diffusivities, the hydraulic gradients do not switch direction with the diurnal stream stage fluctuations (see Figure 3), as may occur in flatter and more homogeneous aquifers.

The average radon concentrations increased with distance from the dead-ice body at the three measurement locations on gaining stream reaches (S1, S5, and S6). This trend would seem to suggest either that the groundwater exchanges with the stream more slowly in the lower parts of the forefield than in the upper regions, or that water infiltrates in the upper parts of the forefield and travels downward. The latter explanation is consistent with the results found by Ward *et al.* (1999). However, the hydraulic conductivities that we have measured at our sites imply long time scales for down-valley groundwater transport (roughly 104 days to travel the distance of about 700 m from the dead-ice body to the farthest downstream transect). This estimate is calculated from the average down-valley gradient (~0.12 m/m), the averaged measured saturated hydraulic conductivity (14 m/day, geometric mean), and the measured porosity (0.25) of the sediments on the forefield. Because radon concentrations in groundwater would reach equilibrium on timescales shorter than this, we assume that down-valley groundwater transport could account for only a small fraction of the water reaching any of the transects.

Our geophysical surveys did not provide precise information about the thickness of the saturated zone. Nevertheless, we can calculate a range of hydraulic transmissivities ($T = Kb = DS$) directly from the calibrated hydraulic diffusivities (114–1156 m^2/day) and the till porosity (0.25). By multiplying the hydraulic transmissivities (29–289 m^2/day) with the approximate surface gradient (~0.12 m/m) and width (~400 m) of the forefield, we obtain an estimate of the groundwater flow through the aquifer (16–161 l/s). This flow rate is 1–8 % of the average stream discharge measured at site S7 during the period from mid June to mid October. The estimated groundwater flow rate is comparable to the base flow in the streams during late autumn (~35 l/s and ~100 l/s measured at site S7 in December 2011 and in October 2010, respectively). The estimated flow through the aquifer is low and indicates that not much water should bypass the stream gauging station near the catchment outlet. This conclusion is plausible since the total stream discharge over the season appears to equal the contributions from snowmelt, glacier melt, and rainfall (Kormann, 2009).

In general, the one-dimensional diffusion model reasonably captured the timing of the groundwater fluctuations at the flatter locations (S1, S3, and S6). However, the amplitudes were not correctly simulated at two of those sites (S3 and S6). The simulation accuracy varied, not only between the sites, but also between the study periods for the individual locations. In particular, for the two upstream sites (S1 and S3), the simulations showed larger deviations from the observations during early summer (T3) than later during the season (T1 and T2). Several factors can contribute to the difference between the observed and modelled groundwater fluctuations; the most influential factors likely include (1) stage-dependent variations in hydraulic connections between the stream and monitoring wells, not considered in the modelling, (2) unrepresentative amplitudes of the stream stage fluctuations used as forcing data, (3) incorrect parameter values used in the simulations, and (4) complex groundwater flows not described by the diffusion model.

The simulation results show that stream-groundwater interactions in such complex terrain as our field site cannot be fully described by the one-dimensional diffusion model. The model seems unable, at least with the available input data, to accurately reproduce the groundwater fluctuations in some places and during some periods. Nevertheless, the model provides valuable insights into how stream stage fluctuations propagate into the riparian zone. In spite of many model simplifications, the inverse modelling approach produced realistic values for hydraulic diffusivity. This result suggests that diffusive processes strongly influence the propagation of stream stage fluctuations into the riparian zone on the forefield.

SUMMARY AND CONCLUSIONS

Seasonal and diurnal variations in stream stage and riparian groundwater levels were measured at four sites in the Damma glacier forefield in central Switzerland. Diurnal fluctuations in riparian zone groundwater levels lagged behind the glacier melt-driven stream stage variations at both loosing and gaining channels. The time lag of the groundwater fluctuations increased with distance from the stream, but their amplitudes did not typically follow the simple pattern predicted by diffusive wave propagation. The time lags and amplitude damping varied greatly between the sites, highlighting the heterogeneity of the glacier forefield. Elevated radon concentrations in groundwater wells located just a few meters from the stream showed that riparian groundwater was not rapidly mixing with stream water on daily time scales, despite the clear diurnal cycles in both stream stage and groundwater levels. The slow diurnal exchange of water between the stream and riparian zone likely occurs because the hydraulic gradients do not switch direction with the diurnal stream level fluctuations.

To describe the groundwater fluctuations, we used a diffusion model which has so far been applied to much flatter regions (e.g. coastal areas). At the three flatter measurement sites on the forefield, the model could reasonably capture the timing of the groundwater fluctuations (but not the amplitudes at two of those sites). Several factors can contribute to the difference between the observed and modelled results, such as inaccurate forcing data and complex groundwater flows not represented in the model. This last factor is probably particularly important at the fourth and steepest measurement location. At this site the model failed to reproduce the observed groundwater fluctuations, partly because of fast groundwater flows in the vicinity of the monitoring wells. Our results show that the causes of diurnal groundwater fluctuations on the forefield are far more complex than in simpler systems (see Montalto *et al*., 2007, Loheide and Lundquist, 2009).

The diffusion model reproduced some key features of the groundwater fluctuations at the flatter observations sites, but could not capture all processes fully. Nevertheless, calibration of the model seems to yield realistic estimates of the hydraulic diffusivity for those sites. The calibration gives an estimate of hydraulic properties for a rather large area, which is particularly useful for heterogeneous field sites. Typically, the variability in estimates of hydraulic properties decreases with increasing sample volume (Mohanty *et al*., 1994). More work is needed to further test methods for inferring hydraulic diffusivity from observations of water level fluctuations, which have previously been used in much flatter regions.

ACKNOWLEDGEMENTS

Financial support for this study was provided by the BigLink project of Competence Centre for Environment and Sustainability (CCES) of the ETH Domain. Henning Löwe deserves gratitude for giving much helpful advice. We also thank the students and staff who helped during the field work and Rienk Smittenberg who contributed with data on sediment properties. Masaki Hayashi thanks the Swiss Federal Institute of Aquatic Science and Technology (Eawag) for providing a research fellowship. The recommendations given by three anonymous reviewers improved the manuscript greatly.

REFERENCES

Aragon-Jose AT, Robbins GA. 2011. Low-flow hydraulic conductivity tests at wells that cross the water table. *Ground Water* **49**: 426–431.

ASCE. 1996. *Hydrology Handbook*. American Society of Civil Engineers: New York; 800.

Bernasconi SM, BigLink consortium. 2011. Chemical and biological gradients along the Damma Glacier soil chronosequence (Switzerland). *Vadose Zone Journal* **10**: 867–883.

Binkhorst GK, Robbins GA. 1998. Conducting and interpreting slug tests in monitoring wells with partially submerged screens. *Ground Water* **36**: 225–229.

Boulton G, Zatsepin S. 2006. Hydraulic impacts of glacier advance over a sediment bed. *Journal of Glaciology* **52**:497–527.

Bouwer H, Rice RC. 1976. Slug test for determining hydraulic conductivity of unconfined aquifers with completely or partially penetrating wells. *Water Resources Research* **12**:423–428.

Butler JJ. 1998. *The Design, Performance, and Analysis of Slug Tests*. Lewis Pub: Boca Raton, Florida; 252.

Cardenas MB. 2010. Lessons from and assessment of Boussinesq aquifer modeling of a large fluvial island in a dam-regulated river. *Advances in Water Resources* **33**: 1359–1366.

Cooper RJ, Wadham JL, Tranter M, Hodgkins R, Peters NE. 2002. Groundwater hydrochemistry in the active layer of the proglacial zone, Finsterwaldbreen, Svalbard. *Journal of Hydrology* **269**: 208–223.

Cooper RJ, Hodgkins R, Wadham JL, Tranter M. 2011. The hydrology of the proglacial zone of a high-Arctic glacier (Finsterwaldbreen, Svalbard): Sub-surface water fluxes and complete water budget. *Journal of Hydrology* **406**: 88–96.

Crossman J, Bradley C, Boomer I, Milner AM. 2011. Water flow dynamics of groundwater-fed streams and their ecological significance in a glacierized catchment. *Arctic, Antarctic, and Alpine Research* **43**: 364–379.

Fairchild IJ, Killawee JA, Sharp MJ, Spiro B, Hubbard B, Lorrain RD, Tison JL. 1999. Solute generation and transfer from a chemically reactive alpine glacial-proglacial system. *Earth Surface Processes and Landforms* **24**(13): 1189–1211.

Francis BA, Francis LK, Cardenas MB. 2010. Water table dynamics and groundwater-surface water interaction during filling and draining of a large fluvial island due to dam-induced river stage fluctuations. *Water Resources Research* **46**: W07513.

Fritz BG, Arntzen EV. 2007. Effect of rapidly changing river stage on uranium flux through the hyporheic zone. *Groundwater* **45**: 753–760.

Hinton MJ, Schiff SL, English MC. 1993. Physical properties governing groundwater flow in a glacial till catchment. *Journal of Hydrology* **142**: 229–249.

Hoehn E, Vongunten HR. 1989. Radon in groundwater - A tool to assess infiltration from surface waters to aquifers. *Water Resources Research* **25**: 1795–1803.

Irvine DJ, Brunner P, Franssen HJH, Simmons CT. 2012. Heterogeneous or homogeneous? Implications of simplifying heterogeneous streambeds in models of loosing streams. *Journal of Hydrology* **424–425**: 16–23.

Jobard S, Dzikowski M. 2006. Evolution of glacial flow and drainage during the ablation season. *Journal of Hydrology* **330**(3–4): 663–671.

Kormann C. 2009. Untersuchungen des Wasserhaushaltes und der Abflussdynamikeines Gletschervorfeldes. Master's thesis, TU Dresden.

Lagarias JC, Reeds JA, Wright MH, Wright PE. 1998. Convergence properties of the Nelder-Mead simplex method in low dimensions. *SIAM Journal on Optimization* **9**: 112–147.

Langston G, Bentley LR, Hayashi M, McClymont AF. 2011. Internal structure and hydrological functions of an alpine proglacial moraine. *Hydrological Processes* **25**: 2967–2982.

Loheide SP, Lundquist JD. 2009. Snowmelt-induced diel fluxes through the hyporheic zone. *Water Resources Research* **45**: 9.

Magnusson J, Farinotti D, Jonas T, Bavay M. 2011. Quantitative evaluation of different hydrological modelling approaches in a partly glacierized Swiss watershed. *Hydrological Processes* **25**: 2071–2084.

Magnusson J, Jonas T, Kirchner JW. 2012. Temperature dynamics of a proglacial stream: Identifying dominant energy balance components and inferring spatially integrated hydraulic geometry. *Water Resources Research* **48**: 16.

Mohanty BP, Kanwar RS, Everts CJ. 1994. Comparison of saturated hydraulic conductivity measurement methods for a glacial-till soil. *Soil science society of American Journal* **58**: 672–677.

Montalto FA, Parlange JY, Steenhuis TS. 2007. A simple model for predicting water table fluctuations in a tidal marsh. *Water Resources Research* **43**: 22.

Nielsen P 1990. Tidal dynamics of the water-table in beaches. *Water Resources Research* **26**: 2127–2134.

Raubenheimer B, Guza RT, Elgar S. 1999. Tidal water table fluctuations in a sandy ocean beach. *Water Resources Research* **35**: 2313–2320.

Rohde A, Seibert J. 2011. Groundwater dynamics in a till hillslope: flow directions, gradients and delay. *Hydrological Processes* **25**: 1899–1909.

Roy JW, Hayashi M. 2009. Multiple, distinct groundwater flow systems of a single moraine-talus feature in an alpine watershed. *Journal of Hydrology* **373**: 139–150.

Smittenberg RH, Gierga M, Göransson H, Christl I, Farinotti D, Bernasconi SM. 2012. Climate-sensitive ecosystem carbon dynamics along the soil chronosequence of the Damma glacier forefield. Switzerland. *Global Change Biology*, doi: 10.1111/j.1365-2486.2012.02654.x

Sun HB. 1997. A two-dimensional analytical solution of groundwater response to tidal loading in an estuary. *Water Resources Research* **33**: 1429–1435.

Vogt T, Hoehn E, Schneider P, Freund A, Schirmer M, Cirpka OA. 2010. Fluctuations of Electrical Conductivity as a Natural Tracer for Bank Filtration in a Losing Stream. *Advances in Water Resources* **33**(11): 1296–1308.

Warburton J 1992. Observations of bed-load transport and channel bed changes in a proglacial mountain stream. *Arctic and Alpine Research* **24**(3): 195–203.

Ward JV, Malard F, Tockner K, Uehlinger U. 1999. Influence of ground water on surface water conditions in a glacial flood plain of the Swiss Alps. *Hydrological Processes* **13**: 277–293.

